Langmuir

Article

pubs.acs.org/Langmuir

Adsorption of Lysozyme on Silver and Its Influence on Silver Release

Xin Wang,*[,†] Gunilla Herting,[†] Inger Odnevall Wallinder,[†] and Eva Blomberg*[,†,‡]

[†]KTH Royal Institute of Technology, School of Chemical Science and Engineering, Division of Surface and Corrosion Science, Drottning Kristinas väg 51, SE-100 44 Stockholm, Sweden

[‡]SP Technical Research Institute of Sweden, Chemistry, Materials and Surfaces, P.O. Box 5607, SE-114 86 Stockholm, Sweden

ABSTRACT: Silver is increasingly used in antimicrobial coatings of biomedical devices and implants to hinder infections. As proteins have been shown to largely influence the extent of released metals from various metal surfaces at biological conditions, silver may also be influenced in the same way. The aim of this study is to relate the structure of adsorbed lysozyme (LSZ) to the release of silver from metallic silver surfaces. Simultaneous adsorption measurements were performed in real time on the same surface using combined ellipsometry and quartz crystal microbalance with dissipation monitoring measurements to provide a more comprehensive understanding on the adsorption kinetics and the layer structures. The concentration of LSZ in 0.15 M $NaNO_3$ solution (pH 7, 25 °C) influences the structure of the adsorbed layer. Monolayer coverage is obtained at concentrations ≤0.1 g/L, while a bilayer structure with a rigid inner layer and a relatively loosely adsorbed outer layer is formed at 1 g/L. The inner layer of LSZ is assumed to bind firmly to silver via disulfide bridges, which makes it irreversibly adsorbed with respect to dilution. The amount of released silver is further influenced by the structure of the LSZ layer. At low LSZ concentrations (≤0.1 g/L) the amount of released silver is not significantly different compared with non-protein-containing $NaNO_3$ solutions; however, noticeable reduction was observed at higher concentrations (1 g/L). This reduction in silver release has several possible explanations, including (i) surface complexation between LSZ and silver ions that may result in the incorporation of silver in the irreversible adsorbed layer and, hence, reduce the amount of released silver into solution, and (ii) net charge reversal at the protein/solution interface to slightly positive surface potentials. Any release of silver will therefore exhibit an electrostatic repulsion during transportation through the protein layer results in a reduced amount of silver in solution.

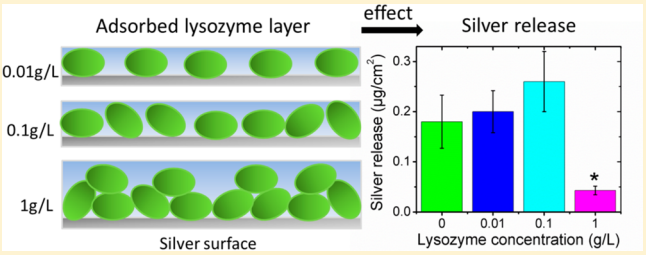

1. INTRODUCTION

Silver has been recognized for its beneficial properties for a long time. In recent years the number of applications has increased due to its broad spectrum of antimicrobial properties.[1−3] Because of the rapid development of nanotechnology, the use of silver has accelerated in medical and biomedical applications, for air and water purification, in food manufacturing, in cosmetics, in clothing, and in a number of household products (such as refrigerators). It has been shown that the antimicrobial properties to a large extent derive from the release of silver ions from the silver-containing product.[2−4] In biomedical applications silver has mainly been used as an active species incorporated in antibacterial coatings on biomaterials and in wound dressings. Antibacterial biomaterial surfaces should not cause any adverse effects on cells, tissues, or fluids (e.g., blood, tears). However, since silver is increasingly used to hinder bacterial infections, widespread silver resistance that may cause adverse effects on humans and the ecosystem is of increasing concern.[2,3]

Antibacterial coatings in biomedical applications may *in vivo* be compromised by protein adsorption that influences the kinetics of the silver release and provides a platform for bacterial attachment at the adsorbed protein layer.[3] It is well known that spontaneous and nonspecific adsorption of proteins in solution will take place in contact with a surface due to the heterogeneous molecular surface of proteins that consists of hydrophobic and hydrophilic patches with positive and negative charges, dipoles, and hydrogen-bonding groups.[5−7] The interaction between a protein and a foreign surface hence becomes anisotropic and often very complex. Proteins interact generally with the surrounding environment via a combination of simultaneously acting intermolecular forces of various origins. Which proteins are preferentially adsorbed and their conformations on the surface are decisive for biocompatibility. Protein adsorption, as the first step of protein−metal interaction, has been extensively studied on model surfaces (e.g., silica, polymeric and thiolated gold), and some general predictions on how and if a protein adsorbs onto a surface can be made from its charge and the surface charge, the structural stability of the protein, and the surface wettability.[5] However, because of its specificity and complex structure, each protein molecule may exhibit its own "personality".[7] Corresponding systematic studies on metallic surfaces are generally lacking. However, studies exist of the adsorption of different proteins on

Received: August 8, 2014
Revised: October 31, 2014
Published: October 31, 2014

titanium, chromium metal, and stainless steel,[8−10] which all are relatively non-reactive (passive) surfaces, but relatively few studies are available on silver surfaces. Previous findings have shown the presence of proteins in solution, and adsorbed on metal surfaces, to influence the extent of metal release in biological media.[8,11] The results clearly show that the net charge of the protein affects the metal release process for passive metal surfaces such as chromium and stainless steel. Negatively charged serum albumins significantly enhanced the release of iron and chromium from stainless steel (up to 40-fold increase), whereas positively charged lysozyme (LSZ) revealed a minor effect.[8] Recent findings on positively charged mussel proteins adsorbed in multilayers on stainless steel show inhibited dissolution of iron and chromium ion at pH 7.8.[12]

The aim in this work is to thoroughly elucidate protein adsorption onto silver and how the structure, rigidity, and solvent content of the adsorbed protein layer influence the silver release in order to elaborate mechanisms for protein-influenced metal release. LSZ was used as a model protein, being a small compact globular protein (3 × 3 × 4.5 nm) of high internal conformation stability that carries a net positive charge at physiological pH.[13] LSZ exists in almost all body fluids in different concentrations, 7−13 mg/L in serum and 1.2 g/L in tear fluids.[14] Its adsorption properties were studied by means of quartz crystal microbalance with dissipation monitoring (QCM-D) and ellipsometry. The novel approach in this study is simultaneous real-time ellipsometry and QCM-D measurements on the very same surface that provide a comprehensive understanding on the adsorption kinetics of LSZ on silver and its layer structure. The sensed mass ("wet mass") received by QCM-D includes the trapped solvent in the layer, whereas the adsorbed amount ("dry mass") is measured with ellipsometry. The combination of these techniques allows an in-depth evaluation of the layer structure, including the relative solvent content associated with layer, the effective density, and the viscoelastic properties of the films. The influence of LSZ adsorption on the release of silver was quantitively determined by means of graphite furnace atomic absorption spectroscopy (GF-AAS).

2. EXPERIMENTAL SECTION

2.1. Chemicals and Solution Preparation. Purified protein lysozyme (LSZ) (L6876) and ultrapure sodium nitrate (≥99.999%) for the adsorption studies and sodium nitrate (≥99.5%) for the silver release studies were purchased from Sigma-Aldrich. All aqueous solution is prepared using ultrapure water (18.2 MΩ cm, Millipore, Sweden).

In the experiment, 0.15 M sodium nitrate ($NaNO_3$) was prepared as background solution from which a series of LSZ solutions were prepared with concentrations ranging from 0.01 to 1 g/L. NaOH (1 vol %) was used to adjust the pH to 7.0 ± 0.1 of the prepared solutions. 0.15 M $NaNO_3$ was used as electrolyte to avoid interference and precipitation of AgCl complexes and to keep the ionic strength in the solution comparable to that of Cl in PBS saline buffer. When considering the range of the electrostatic interactions any difference between the use of Cl^- and NO_3^- would not be observed since both ions are monovalent and, hence, the ionic strength will be the determining parameter for the screening length. If specific ion effects are taken into account, the choice of ions might influence the solubility/adsorption of the protein. The selection of Cl^- would in that case be more realistic for physiological conditions. However, recent studies have shown that any prediction on the adsorption of proteins made from the type of salt, of the same valence state, is rather difficult.

2.2. Substrates. QCM-D measurements were performed using evaporated silver surfaces, AT-cut 5 MHz quartz crystals deposited with 100 nm silver (QSX 322) purchased from Biolin Scientific, Sweden, with a surface area of approximately 1.5 cm^2. Massive silver coupons, sized approximately 5 cm^2 (metal release), were abraded using 1200 SiC grade paper (1600 μm) and pre-aged for 24 h after cleaning. This was done to ensure comparable and reproducible initial surface characteristics. Prior to use, massive and silver-coated surfaces were cleaned by isopropanol followed by absolute ethanol and finally rinsed in Milli-Q.

The coated silver crystals reveal a static contact angle of approximately 60−70° when measured by the sessile drop method (Pocket Goniometer, Fibro System, Sweden). Even though these surfaces are slightly hydrophobic, they are negatively charged at pH 7 and show an isoelectric point (iep) between pH 5 and 6 (see Figure 1 below). The measured iep for the massive silver was slightly lower, pH 4−5, and slightly more hydrophobic, although the measured zeta potential at pH 7 was the same (−30 mV) as for the silver-coated QCM crystal (data not shown).

2.3. Zeta Potential Measurements. An electrokinetic analyzer (SurPASS, Anton Paar GmbH, Graz, Austria) was used to measure the surface potential of silver-deposited QCM surfaces for adsorption measurements (Figure 1) and of the massive silver coupons used for silver release measurements. Detailed information on the instrumental technique and setup is given elsewhere.[15,16] For the QCM surfaces, an adjustable-gap cell for circular discs with a diameter of 1.4 cm was used, and the variable separation between the two silver surfaces was set to approximately 120 μm. Solution flow was induced in the measurement cell by ramping the differential pressure from 0 to 300 mbar in both flow directions. Two cycles of pressure ramping in each direction were carried out, and the average values for all four cycles were used to calculate the average zeta potential. The zeta potential was obtained from the Smoluchowski equation by measuring the change in streaming current versus the applied differential pressure.[16] A 1 mM $NaNO_3$ solution was used as the electrolyte, and HNO_3 (0.1 M) and NaOH (0.1 M) were used to adjust the solution pH in the range between 2 and 10. Two separate pH titration curves and two single-point measurements were performed on fresh surfaces.

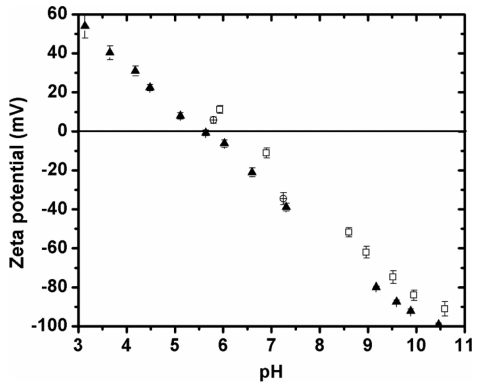

Figure 1. Zeta potential, based on at least duplicate measurements, as a function of pH in 1 mM $NaNO_3$ for silver deposited QCM crystals. Triangles and squares represent two separate pH titrations on two different surfaces, circles represent two separate single-point measurements on fresh surfaces. Error bars correspond to the deviation between four measuring cycles.

Metal and/or metal oxide surfaces in water/electrolyte solutions become charged by adsorption or desorption of potential determining ions. A thin layer of reversible adsorbed oxygen is present on the silver surface[17,18] as no oxide, e.g., Ag_2O, is stable in water solutions (pH < 12). The presence of physisorbed water has been confirmed by recent Raman measurements.[19]

2.4. Quartz Crystal Microbalance with Dissipation Monitoring (QCM-D). 100 nm silver-coated AT-cut quartz crystals (QSX 322, Q-sense AB, Sweden) were used as the substrate to conduct the measurement by QCM-D E4 and QCM-D E1 (Q-sense AB, Sweden) at 25 °C with a flow rate of 200 μL/min.

dx.doi.org/10.1021/la503170x | Langmuir 2014, 30, 13877−13889

Changes in the resonance frequency (Δf) and energy dissipation (ΔD) were monitored by multiple odd overtones with a fundamental frequency of 5 MHz.[20] The sensed mass of adsorbed protein layers was estimated using both the Sauerbrey equation[21] and the Voigt model[22] supplied by Q-tools (Q-sense AB, Sweden).

The Sauerbrey equation is used for calculating the sensed mass of the rigid film with no energy dissipation, while the Voigt model takes into account viscoelastic properties of the layer and is generally used to calculate the sensed mass of "soft" layer.[22,23] Energy dissipation of the silver deposited crystal oscillation reveals the layer viscoelastic properties.

2.5. Ellipsometry. Ellipsometry measurements were conducted using a Q-Sense ellipsometry module system (Q-sense AB, Sweden), which is a module that combines a Null ellipsometer with a Q-Sense E1 system and enables simultaneous QCM-D and ellipsometric measurements on the same substrate. A Multiskop instrument (Optrel GdBR, Berlin, Germany) equipped with a 532 nm laser (Nd:YAG laser) was used for the ellipsometry measurement. Null ellipsometry was used to follow the time evolution of the sample to monitor the kinetics of the adsorption process on the silver substrate (QSX 322, Q-sense AB, Sweden) at an incidence angle of 65°. Ellipsometric angles (Δ and Ψ) were continuously recorded in situ every 10 s.

The adsorbed amount was evaluated using de Feijter's formula:[24]

$$\Gamma = \frac{d_A(n_A - n_C)}{dn/dc} \quad (1)$$

where d_A is the thickness of the adsorbed protein layer. n_A and n_C are refractive indices of the adsorbed protein molecules and the buffer, corresponding to assumed values of 1.48 and 1.33, respectively.[25] dn/dc is the refractive index increment of the molecules, with a value of 0.186 ± 0.003 cm^3/g.[24] It has been shown for thin films adsorbed onto metal surfaces (i.e., gold) that the Drude equation fails in determining the refractive index of thin film due to the presence of thin light-adsorbing regions at the interface between the dielectric film and the metal. This explanation seems likely for protein film adsorbed on a silver surfaces, owing to the common noble character of these two metals.[26] Hence a fixed value of the refractive index for the protein films was used for calculating the adsorbed amount of LSZ.

Based on the sensed mass obtained by QCM-D and the adsorbed amount of LSZ obtained from ellipsometry, the solvent content was calculated as[27]

$$w_{solvent}(\%) = \frac{m_{QCM} - \Gamma_{ellip}}{m_{QCM}} \times 100 \quad (2)$$

2.6. Silver Release Measurements. *2.6.1. Measurements with Different Exposure Times and LSZ Concentrations.* Abraded and cleaned (cf. section 2.2) massive silver coupons were exposed to pure 0.15 M $NaNO_3$ (NA) and 1g/L LSZ-containing NA solution for 2, 4, 8, and 24 h, respectively, at 25 ± 0.1 °C in an incubator (Platform-Rocker incubator SI80, Stuart). In order to investigate the effect of protein concentration on the amount of released silver, immersion experiments were also conducted in series with protein concentration ranging from 0.01 to 1 g/L for 2 and 24 h. The ratio of surface area/solution volume was kept constant at 1 cm^2/mL. After exposure, the coupons were removed from the test vessels, rinsed with ultrapure water, dried by N_2 gas, and stored in a desiccator. The remaining solution in the vessels was acidified to pH 2 for conservation and further metal release analysis. Triplicate samples and one blank (solution only) were exposed in parallel to enable statistical evaluation of the data.

All vessels and tools were acid-cleaned in 10% HNO_3 for at 24 h, rinsed four times in ultrapure water, and dried by N_2 gas to avoid metal contamination.

2.6.2. Measurements in Different Solution Sequences. Massive silver coupons was alternately exposed to $NaNO_3$ (NA) and/or LSZ (1g/L) solution (pH 7) to investigate the influence of LSZ on the silver release process. Coupons were consecutively exposed to six different solutions (each for 30 min). The coupons were directly taken out from the solution and positioned into the next solution (fresh $NaNO_3$or LSZ) as schematically illustrated in Figure 2. Four different exposure sequences were studied: (i) pure 0.15 M $NaNO_3$ (NA-NA-NA-NA-NA-NA), (ii) 0.15 M $NaNO_3$ with 1 g LSZ/L (LSZ-LSZ-LSZ-LSZ-LSZ-LSZ), (iii) alternatively to LSZ and pure $NaNO_3$ solutions (LSZ-NA-LSZ-NA-LSZ-NA), and (iv) alternatively to LSZ, pure $NaNO_3$ and pure $NaNO_3$ solutions (LSZ-NA-NA-LSZ-NA-NA). The release of silver was determined for each step of each sequence after solution acidification to pH 2. Triplicate samples and one blank (solution only) were exposed in parallel for each step and sequence to ensure the reliability of the results.

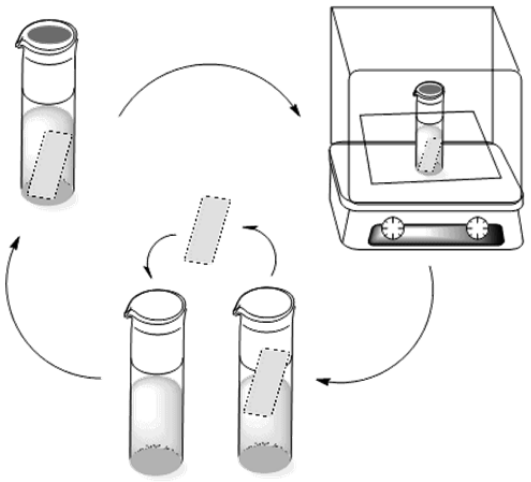

Figure 2. Schematic illustration of consecutive sequential exposure procedure in $NaNO_3$/LSZ solutions (25 °C and pH 7) to assess the release of silver from massive silver coupons.

2.6.3. Silver Release Analysis. Previous to graphite furnace atomic absorption spectrometry (GF-AAS, Perkin Elmer Analyst 800) all measured solutions were pretreated by UV digestion (705 UV Digester, Metrohm) in order to exclude interference of silver complexes and ensure total silver analysis. The procedure was performed in three steps to ensure complete destruction of complexes by adding 250 μL of H_2O_2, 6.6 mL of ultrapure water, and 150 μL of HCl (30%) to 2 mL of sample solution followed by a 30 min digestion. The second step included the addition of 1 mL of H_2O_2 and digestion for another 30 min, directly followed by the last step with the addition of another 1 mL of H_2O_2 and digestion for 60 min. This resulted in a total dilution factor 5.5. The digested solutions were allowed to cool to ambient laboratory temperature and kept in acid-cleaned containers for GF-AAS analysis. The final volumes were recorded for the calculation of the original silver concentration. Ultrapure water (0 μg/L) and four silver standards, 7.5, 15, 30, and 45 μg/L, were prepared for the AAS calibration. All measured concentrations of silver for each solution (each step in the sequence, triplicate samples) were based on triplicate readings. The limit of detection (LOD) was determined by the method of Vogelsang and Hädrich[28] based on the calibration curve and the measurements at the standard concentrations used for calibration (0, 7.5, 15, 30, and 45 μg/L) in each matrix solution. The method considers the grade linearity, matrix effects, and recovery of the samples. The LOD was determined to be 2.1 and 2.7 μg/L in $NaNO_3$ and LSZ solutions, respectively. All reported values are above the LOD. Corresponding limits of quantification (LOQs) were determined to be 7.4 and 9.1 μg/L, respectively. All results are reported as the mean value of replicate samples, shown as

$$\bar{x} = \frac{1}{3}\sum_{i}^{n}((x_i - x_B)f_n) \quad (3)$$

where x_i is the individual sample value, x_B is the value of the blank, f_n is the factor of diluted volume, and n is the number of exposed samples. Generated results are expressed as the amount of released silver per geometric surface area (μg/cm^2) and the rate of released silver per surface area and per hour (μg/cm^2/h).

dx.doi.org/10.1021/la503170x | Langmuir 2014, 30, 13877−13889

3. RESULTS AND DISCUSSION

3.1. LSZ Readily Adsorbs on Silver and Forms an Irreversibly Adsorbed Inner Layer and a Relatively Loosely Adsorbed Outer Layer at High Concentrations.

The adsorption of LSZ (1 g/L) in 0.15 M $NaNO_3$ (pH 7, 25 °C) onto a 100 nm silver-coated crystal surface was monitored in real-time by means of QCM-D. Shifts in frequency (Δf) and dissipation (ΔD) are illustrated in Figure 3 as a function of time.

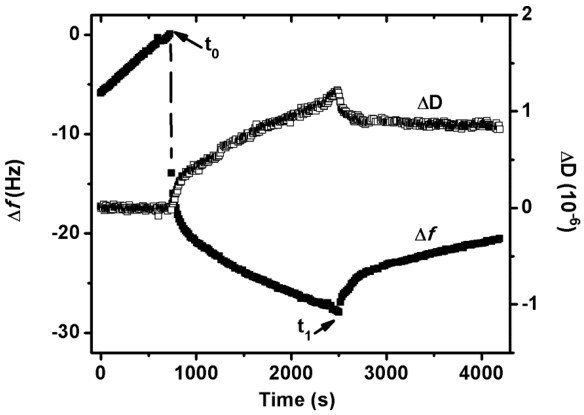

Figure 3. Adsorption of LSZ (1g/L) onto silver at pH 7 and 25 °C measured by means of QCM-D. Changes in frequency (Δf) and dissipation (ΔD) are displayed as a function of time, with overtone 5 taken as an example. LSZ+$NaNO_3$ solution was injected at t_0 followed by a subsequent rinse with protein-free $NaNO_3$ solution at t_1.

The arrows display the injection (t_0) of LSZ + $NaNO_3$ and the subsequent rinse (t_1) with protein-free $NaNO_3$. Δf shifts sharply down to about 17 Hz, which reflects LSZ adsorption. This process takes place within a few seconds from injection (t_0) and results further in an increased shift in the recorded ΔD, which indicates a high affinity type adsorption.[29] This is followed by a concomitant gradual reduction in Δf and a continued increase in ΔD with time, which imply further adsorption of LSZ. Adsorption of LSZ onto the silver surface shows similar trends as previously observed for chromium and stainless steel surfaces, but quite different compared with the adsorption of the negatively charged and flexible bovine serum albumin (BSA) protein, for which adsorption equilibrium takes several minutes to reach.[8,11] Such differences are explained by the fact that protein adsorption both depends on the its properties and on the surface characteristics, e.g., surface charge, protein charge, and conformational stability.[30] At pH 7, LSZ is net positively charged (derives from a surplus of positively charged amino acids at the protein surface), and the silver-coated crystal surface is negatively charged (see Figure 1). Electrostatic interactions are hence an important driving force for LSZ surface adsorption. Calculations of the number of positively charged amino acids at the surface of chicken egg lysozyme (data taken from the Protein Data Bank, PDB 1HEL) reveal that all lysine (Lys) and approximately 60% of the arganine (Arg) present in the amino acid sequence actually are located at the protein surface. Previous studies of amino acid adsorption onto negatively charged stainless steel surfaces show high adsorption affinities at pH 7 for both Lys and Arg.[31] These amino acids are hence also expected to play an important role in the adsorption of LSZ on the negatively charged silver-coated surface. However, as the high ionic strength of the present study (0.15 M), efficiently screening charges of the surface and of LSZ, relatively short-range electrostatic double-layer interactions are possible (Debye length, $\kappa^{-1} = 0.304/C_0^{1/2} = 0.78$ nm, for 1:1 $NaNO_3$).[32] This is confirmed by the lack of significant differences observed for LSZ adsorbed at pH 5 compared with 7 (data not shown). This means further that the entropy gain obtained during protein adsorption (from the release of counterions associated with the protein and the surface, as well as water molecules close to both the protein and the surface) must be considered.[6,33] In contrast to "soft" proteins like albumin, immunoglobulin, and transferrin that all have low internal conformation stabilities, LSZ is a small and rigid protein designated as a "hard" protein with a minor tendency for conformational changes upon surface adsorption.[7] From this it follows that an entropy gain due to conformational changes most likely only contributes to a very small extent to the driving force for LSZ adsorption onto the silver surface. It is well known that sulfur atoms have high chemical affinity to noble metals, e.g., gold and silver, which create strong bonds with sulfur-containing molecules such as thiols and organic disulfides. A recent study by Podstawka et al., who utilized Raman and surface-enhanced Raman scattering (SERS) to investigate the adsorption of proteins containing disulfide bonds onto colloidal silver surfaces, revealed that bonding to the silver surface takes place at disulfide bridges located between Cys(5)-Cys(127) and Cys(30)-Cys(115) in LSZ without any cleavage of the S−S bonds.[34] The same study showed that LSZ did not undergo any denaturation or large conformational change upon bonding to the colloidal silver surface since both amide I and amide II peaks were clearly seen in the SERS spectra. It is hence reasonable to assume that also this kind of binding takes place between LSZ and the silver surface of this study.

Protein-free $NaNO_3$ solution was injected after 2500 s (t_1). The removal of proteins from the solution resulted in an increase in magnitude of Δf and a decrease in ΔD, which imply partial desorption of LSZ from the silver surface (Figure 3). However, most LSZ was irreversible adsorbed, believed to be explained by the strong binding between the silver surface and disulfide bridges of the LSZ molecule, as previously discussed. Irreversible adsorption of proteins with respect to dilution is commonly observed in protein adsorption studies.[6,7,35] This is explained by the numerous contact points between the adsorbed protein molecule and the surface and the fact that all segments have to detach for complete desorption. This results generally in a non-equilibrium irreversible process. The thermodynamic description of protein adsorption/desorption processes should hence in general be based on the laws of irreversible thermodynamics.[6] During the rinsing process, ΔD reaches a constant value while Δf continues to increase. The change in frequency shows a linear change with a slope that is similar to observed linear frequency changes during the initial period of the measurements prior to protein injection, i.e., during rinsing in pure $NaNO_3$ (between 0 min to t_0). Rinsing the exposure chamber by pure $NaNO_3$ in the beginning of each measurement was done to enable a stable baseline, and resulted in a linear increase in Δf with time (Figure 3). This increase in magnitude of the frequency is attributed to the release of silver ions from the silver-coated QCM crystal (discussed later). Two processes take hence place during the rinsing process that results in an increase in magnitude of Δf with time, i.e., desorption of loosely adsorbed LSZ during the initial period of rinsing solution and release of silver ions from the surface.

In order to confirm that the linear increase in magnitude of Δf during rinsing partly is related to the release of silver ions from the underlying surface, Δf was plotted as a function of

dx.doi.org/10.1021/la503170x | Langmuir 2014, 30, 13877−13889

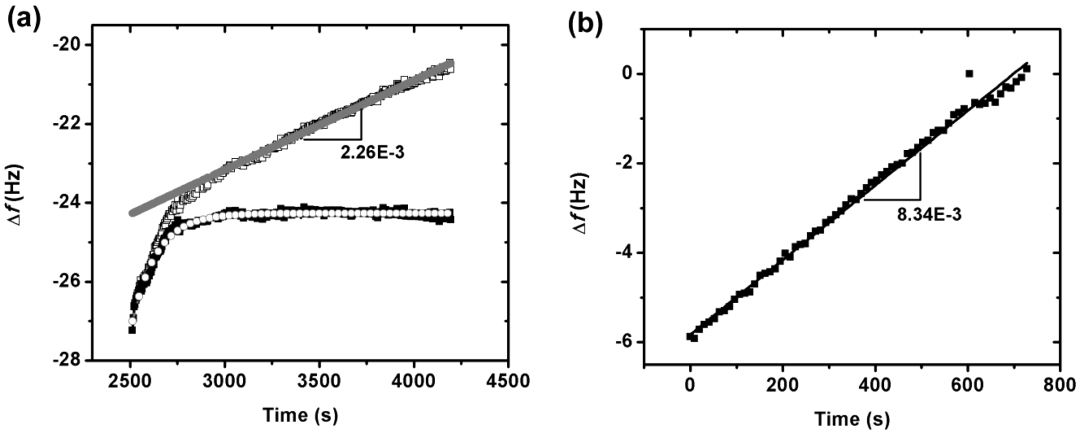

Figure 4. (a) Frequency change (Δf) versus time during rinsing (top curve). The linear part of Δf related to silver release from the coated QCM crystal is subtracted to show the real Δf versus time (bottom curve). (b) Linear changes in Δf upon exposure in pure $NaNO_3$ with time prior to LSZ injection.

time and analyzed by mathematical fittings (Figure 4a). It is clearly seen that after an initial rapid increase in magnitude of Δf, indicative of partial desorption, the measured Δf can be linearly fitted. When subtracting this linear Δf shift from the measured Δf, a frequency plateau is clearly observed after the initial increase in magnitude of Δf, which demonstrates that desorption equilibrium is achieved (Figure 4a). When comparing the linear increase in magnitude of Δf during rinsing (pure $NaNO_3$) with the measured Δf prior to injection of protein into the measuring chamber, it is evident that Δf increases linearly with rinsing time as illustrated in Figure 4b. This indicates a relatively constant release with time of silver ions from the silver-coated crystal. A slightly larger slope during the initial rinsing process with pure $NaNO_3$ compared with the slope after protein injection indicates a faster release of silver ions in pure $NaNO_3$. However, a constant release of silver ions can still be observed after LSZ adsorption onto the silver surface during rinsing in pure $NaNO_3$. This will be discussed in more detail later in section 3.3.

Protein desorption due to partly reversible adsorption of proteins on surfaces is a common phenomenon and well reported for surfaces such as stainless steel,[8,9,11,29] chromium,[11] and silica.[36,37] The amount of desorbed protein from the adsorbed layer is related to the adsorbed amount of the proteins, which in turn is related to the structure of the adsorbed layer, e.g., monolayer vs multilayer coverage. Adsorption studies of LSZ onto negatively charged silica, using dual polarization interferometry (DPI) in high protein concentration solutions, reveal a multilayer structure.[36] Rinsing with a protein-free buffer solution results in partial desorption in cases when the adsorption of LSZ on the silica surface exceeded a monolayer. The reduction in adsorbed mass during rinsing was most significant for LSZ adsorbed in multilayers with an initially higher rate of desorption that leveled off to a steady-state value, closely related to monolayer coverage. These observations are consistent with the observed desorption of LSZ of the present study. After subtraction of the Δf contribution related to the release of silver ions from the underlying silver-coated surface in pure $NaNO_3$, it was evident that the increase in Δf during rinsing took place at a higher rate during the initial period of the rinsing process, followed by steady-state conditions. The exponential pattern reveals that a kinetic desorption process takes place with loosely bound LSZ molecules initially desorbed at a higher rate, and that this rate significantly slows down as the surface concentration of loosely adsorbed molecules is reduced. At given LSZ concentrations (1 g/L), the results indicate that more than one layer of LSZ is adsorbed at the silver surface, and that an inner layer is firmly bound to the surface, even after rinsing. Previous findings have shown that LSZ are present as dimers at high concentrations.[38] Even though LSZ does not form dimers in bulk solution at given concentrations, the existence of a second layer is not surprising at a surface of locally high protein density.[38] As mentioned earlier, may complete desorption only occur if all bonds are broken simultaneously. Such a detachment of all segments requires a substantially higher free energy than what is required for surface binding. Hence, the strong binding of the inner layer of LSZ may, as previously proposed, be partly attributed to the strong bonding between disulfide bridges of the LSZ protein and the silver surface.[34]

3.2. The LSZ Layer Forms a Non-Fully Surface-Covered Rigid Layer at Low Concentrations with Most Molecules Packed Side-On in a Monolayer Arrangement, whereas a Bilayer Conformation Forms at High Concentrations. The influence of LSZ concentration (0.01, 0.1, and 1 g/L) on the adsorption on silver was further investigated at pH 7 by means of QCM-D. The sensed mass of adsorbed LSZ was calculated prior to and after rinsing with NA (pure 0.15 M $NaNO_3$) (Figure 5a). As previously reported, the Sauerbrey equation does not take into account the viscoelastic properties of adsorbed layers and is therefore only applicable for rigid layer calculations, as it underestimates the sensed mass for soft layers.[22,39] If the adsorbed protein layer is soft, Δf and ΔD for different overtones will not overlap (Figure 5b). It is hence evident in this study that the energy dissipation must be taken into account for LSZ concentrations of 0.1 g/L and above, and that the sensed mass should be calculated using the Voigt model. It is clearly seen (Figure 5a) that the sensed mass of LSZ adsorbed onto the silver-coated surface increases when the protein concentration increases from 0.01 to 1 g/L. The results clearly show that LSZ desorbs during rinsing with protein-free electrolyte solution, and that the fraction of desorbed LSZ increases with increasing concentration, findings in line with other studies on LSZ adsorption onto negatively charges silica.[36] The discrepancy in sensed mass calculated using the two models (eq 4, where m_V and m_S denote calculated sensed masses prior to rinsing using the Voigt and the Sauerbrey model, respectively) becomes more obvious with increasing protein concentration.

$$\text{discrepancy (\%)} = \frac{m_V - m_S}{m_S} \times 100\ \% \qquad (4)$$

dx.doi.org/10.1021/la503170x | Langmuir 2014, 30, 13877−13889

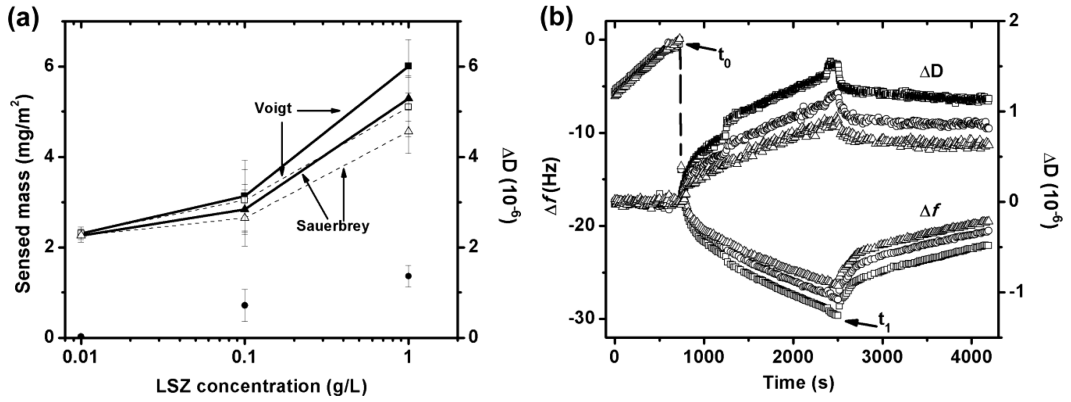

Figure 5. (a) Sensed mass of adsorbed LSZ on a silver-coated surface before (solid lines, filled symbols) and after (dashed lines, unfilled symbols) rinsing with pure $NaNO_3$ solution (0.15 M) as a function of protein concentration (0.01, 0.1, and 1 g/L), calculated by the Voigt model (squares) and the Sauerbrey equation (triangles), and corresponding dissipation changes (ΔD) (solid circles). (b) Changes in frequency (Δf) and dissipation (ΔD) versus time for 1 g/L LSZ at pH 7 and 25 °C illustrated by the response from three random overtones (squares, n = 3; circles, n = 5; triangles, n = 9; f_0 = 5 MHz).

The calculated discrepancy value was small, 2% (m_V = 2.31 mg/m^2, m_S = 2.26 mg/m^2) at the lowest LSZ concentration investigated (0.01 g/L), which indicates a rigid layer, further supported by a small change in energy dissipation (Figure 5a). However, at the highest LSZ concentration (1 g/L), the calculated discrepancy value was almost 14%, and the ΔD increased. This reflects a soft layer with both elastic and viscous dissipative properties, rather than the purely elastic response assumed by the Sauerbrey equation.[39] A softer layer is further supported by the increase in ΔD (Figure 5a) and the deviation between the overtones (Figure 5b). The results clearly show differences in structure of the adsorbed protein layer at different protein concentrations, which may be related to differences in protein diffusion toward the surface. In a more concentrated protein solution the flux toward the surface is higher. This means that a larger number of protein molecules arrive and attach to the silver surface at the same time, from which follows a shorter time for protein relaxation to a more steady-state surface conformation.[35]

Further insight in the adsorption process is provided in Figure 6a, where Δf is plotted against ΔD (removes time as a variable).[39] At 0.01 g/L, the energy dissipation is very low (scattering around zero), and after a rapid adsorption, Δf remains constant (data not shown). The $\Delta D/\Delta f$ value indicates mass addition without significant dissipation increase, which is characteristic of a fairly rigid layer (previously shown in Figure 5a and illustrated via Voigt and Sauerbrey calculations). Rinsing with the protein-free solution resulted in minor desorption of adsorbed LSZ (Figure 5a). LSZ is a globular protein of slightly ellipsoidal shape sized 3 × 3 × 4.5 nm.[13] The maximum theoretically absorbed amount is 2.07 mg/m^2 for a hexagonal close-packed (HCP) monolayer for side-on adsorption of the LSZ molecule, while a randomly sequentially adsorbed (RSA) monolayer corresponds to 1.2 mg/m^2. A total surface coverage by end-on orientated molecules would result in higher adsorbed amounts: 3.10 mg/m^2 for HCP and 1.9 mg/m^2 for RSA.[40] The sensed mass by QCM-D at 0.01 g/L is about 2.3 mg/m^2 (Figure 5a), i.e., only slightly higher compared with the theoretically adsorbed amount for a HCP side-on monolayer of LSZ. It is hence reasonable to assume that LSZ does not fully cover the surface at the low concentrations (0.01 g/L) when considering that the sensed mass obtained from QCM-D technique also includes the mass of trapped solvent, i.e., the solvent associated with and within the adsorbed layer (in the interstices), including the protein hydration layer.[23,36] Similar findings have been reported for LSZ adsorbed on silica based on neutron reflectivity measurements in 10 mM phosphate buffer at pH 7.[37] A concentration of 0.03 g/L LSZ resulted in a side-on monolayer with an adsorbed amount of 1.7 mg/m^2 (not including the mass of trapped solvent) and a fill factor of 0.39, which is slightly lower than the RSA arrangement of molecules on the surface. This was later confirmed by Lu et al., who studied LSZ adsorption onto silica in 10 mM phosphate buffer at pH 7 using DPI.[41]

A ten times higher LSZ concentration (0.1 g/L) resulted in a linear increase in ΔD with Δf after an initial frequency shift (~10 Hz) (Figure 6a). $\Delta D/\Delta f$ deviates somewhat from linearity at the highest LSZ concentration (1 g/L) investigated (a break point in the curve can clearly be seen). It is evident in both cases that the gradients of the linear regions extrapolate to a negative frequency. This is most likely due to a rapid frequency shift due to protein adsorption taking place during in the first seconds of injection, whereas the linear relationship relates to diffusion controlled adsorption from bulk solution.[42] From Figure 6a, it is further evident that the slope is different between the $\Delta D/\Delta f$ curve in 0.1 and 1 g/L LSZ, respectively. The latter shows a changed slope that may indicate that the average structural conformation of the protein layer is altered during the adsorption process, with a less compact and softer layer as a consequence.[39,43] This supports once more previous discussions of the adsorption of a firmly attached inner LSZ layer and a loosely bound outer layer on silver at higher protein concentrations. A similar layer structure with a side-on bilayer has previously been proposed by Su et al. for LSZ (1 g/L) adsorption onto negatively charged silica in 10 mM phosphate buffer at pH 7 using neutron reflection.[37] They observed a significantly lower LSZ molecule density in the outer layer (filling factor of 0.28) compared with the inner layer (0.55), findings consistent with this study. However, a slightly higher filling factor may be expected in this study due to a higher ionic strength, which will reduce lateral repulsion between the adsorbed protein molecules. A lower density of LSZ in the outer layer would give rise to a steeper slope of $\Delta D/\Delta f$ with increased adsorption, i.e., increased change in frequency, as observed in Figure 6a. The same structure with a firmly attached inner layer and a loosely bound outer layer of LSZ has

dx.doi.org/10.1021/la503170x | Langmuir 2014, 30, 13877−13889

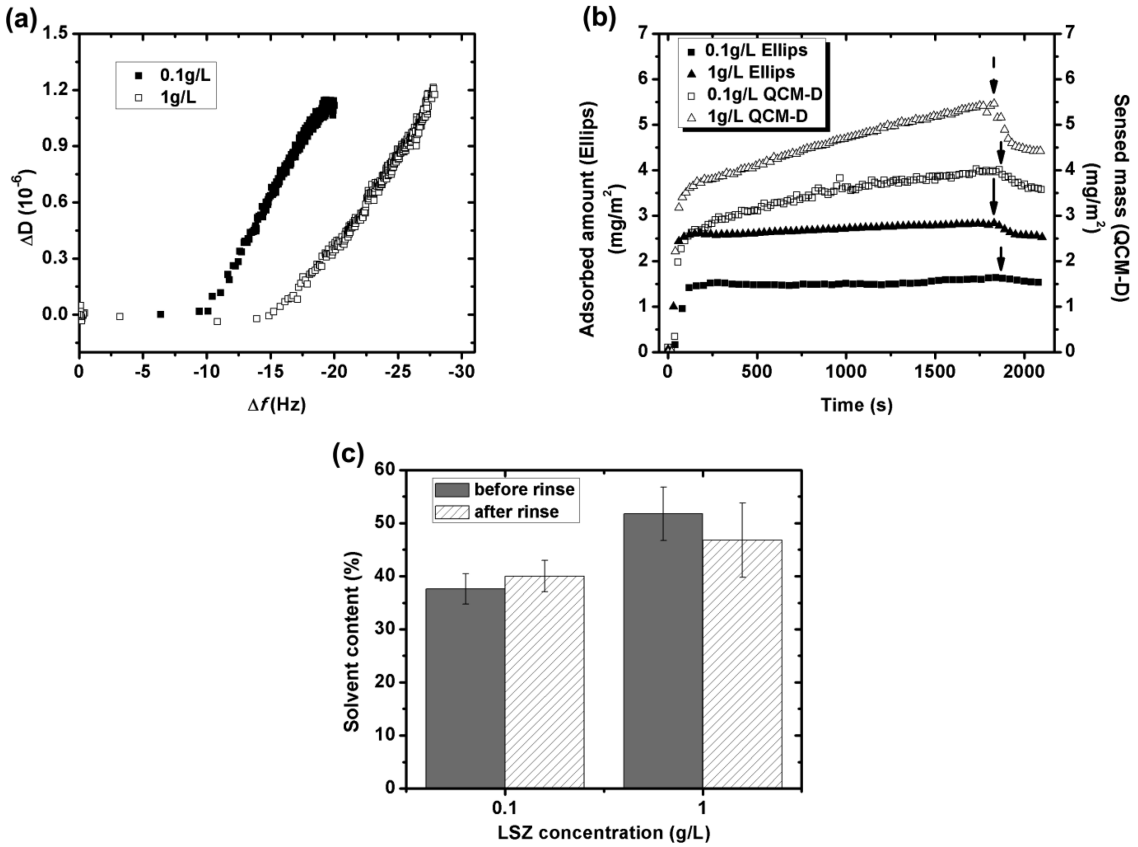

Figure 6. (a) Change in dissipation (ΔD) as a function of change in frequency (Δf) for LSZ adsorption on silver-coated QCM crystals at LSZ concentrations of 0.1 and 1g/L. (b) Changes in mass of adsorbed LSZ determined by means of ellipsometry (Ellips, adsorbed amount) and QCM-D (sensed mass) versus time at 0.1 and 1 g/L. Arrows indicated the beginning of the rinsing cycle, pH 7, T = 25 °C. (c) Solvent content of the LSZ layer adsorbed from 0.1 and 1 g/L, calculated from the sensed mass (QCM-D) and the adsorbed amount (ellipsometry). Error bars represent the deviation between two separate measurements on fresh surfaces; however, the trend before and after rinsing in each separate measurement was the same.

also previously been observed for negatively charged mica by using surface force apparatus measurements.[38,44]

The sensed mass by means of QCM-D does, as mentioned previously, include hydrodynamically trapped solvent associated with and within the adsorbed protein layer. Simultaneous real-time measurements of the adsorbed mass ("dry mass") using an optical technique such as ellipsometry on the very same surface allow for a more detailed interpretation of the layer structure and of its solvent content.[25] The density of a protein layer increases continuously until it reaches the characteristic value for the protein, the surface, and given experimental conditions.[25] The adsorbed amount of LSZ measured by means of ellipsometry and the sensed mass measured using QCM-D were simultaneously determined at the very same silver-coated surface for 0.1 and 1.0 g/L LSZ (Figure 6b). Rapid increases in sensed mass and adsorbed amount are observed at both concentrations, typical for a high affinity type of adsorption. As expected, the adsorbed amount is lower compared with the sensed mass since the adsorbed amount is a measure of the "dry" mass, i.e., without any contribution from the solvent. It is also evident from the figure that the adsorbed amount reaches steady state values after only a few minutes whereas the sensed mass continues to increase over the total measuring period. Since it was found that the silver release from the underlying surface was significantly reduced in the presence of LSZ in solution (section 3.3), the sensed mass was calculated without any correction of Δf. This effect was more pronounced for the highest LSZ concentration (1 g/L). Differences in adsorption profiles might be related in differences to detect the loosely bound outer layer using optical techniques, which uses changes in refractive index of the adsorbing layer to determine the adsorbed mass,[44] whereas QCM-D is able to sense an outer layer of few molecules. Rinsing with LSZ-free $NaNO_3$ does not significantly change the adsorbed amount, while the sensed mass clearly decreases to a larger extent upon rinsing at the higher LSZ concentration. Average adsorbed masses for solutions with 0.1 g/L LSZ were determined with ellipsometry to 1.72 and 1.63 mg/m^2 before and after the rinse, respectively. Corresponding average values at 1 g/L LSZ were 2.75 and 2.52 mg/m^2. When compared with the maximal theoretically adsorbed mass, it is evident that the optical mass at the intermediate LSZ concentration (0.1 g/L) resembles something between a RSA and HCP side-on monolayer, and the highest LSZ concentration (1 g/L) more closely resembles a layer with a mixture of HCP side-on and end-on configurations.[38,44] Monte Carlo simulations of LSZ orientations on charged surfaces have shown that the orientation distribution of adsorbed LSZ molecules become wider, i.e., a more random orientation increases (e.g., side-on and end-on) in solutions of high ionic strength (>0.1 M).[45]

Information of viscoelastic properties of the adsorbed layer can be gained from Voigt fitting of changes in frequency and dissipation.[22] The adsorbed layer was in this study modeled as a

dx.doi.org/10.1021/la503170x | Langmuir 2014, 30, 13877−13889

uniform layer. This means that calculated layer viscosity and layer shear elastic modulus values reflect average (effective) properties of a possibly heterogeneously adsorbed layer. The calculated layer viscosity and layer shear elastic modulus are presented in Table 1 for LSZ concentrations of 0.1 and 1 g/L,

Table 1. Layer Shear Elastic Modulus and Layer Viscosity Values Calculated for the Adsorbed LSZ layer at 0.1 and 1 g/L Prior to and after Rinsing with LSZ-Free $NaNO_3$ Solution[a]

	layer shear modulus ($\times 10^5$ Pa)		layer viscosity ($\times 10^{-3}$ Pa·s)	
LSZ concn (g/L)	before rinse	after rinse	before rinse	after rinse
0.1	7.03 ± 0.29	7.61 ± 0.08	3.92 ± 0.60	4.62 ± 0.55
1	9.15 ± 0.71	19.2 ± 1.31	5.61 ± 1.31	7.74 ± 4.44

[a]Calculations using the Voigt model, overtones 5, 7, and 9, and a fixed density of 1400 kg/m^3.

using a fixed density of 1400 kg/m^3. The results show that both the layer viscosity and the layer shear modulus increase after rinsing with a protein-free solution. This indicates that the layer becomes more rigid during rinsing due to partial desorption of loosely bound LSZ molecules, and that desorption increases with increasing protein concentration. The fact that the layer viscosity and the layer shear modulus increase with increased LSZ concentration indicates a more tightly packed layer at higher concentration,[39] which may be related to a more extensive adsorption of LSZ onto the silver-coated surface (Figures 5a and 6a).

Amounts of solvent associated with and within the layer were calculated from the adsorbed ("dry mass") and sensed mass ("wet mass") using eq 3. The solvent content of the adsorbed layers in 0.1 and 1 g/L LSZ are displayed in Figure 6c before and after rinsing with pure $NaNO_3$.The solvent content was essentially the same for the low LSZ concentration (0.1 g/L) before and after rinsing, whereas an increased solvent content was seen for the higher LSZ concentration (1 g/L). A slight reduction of the solvent content was observed after rinsing even though the deviation between separate measurements cannot be statistically proven the trend before and after rinsing in each separate measurement was the same. This may be explained by partial desorption of the loosely adsorbed outer layer, that may result in a somewhat smoother outermost surface. A solvent content of 40−50% of the adsorbed LSZ layers in this study is consistent with findings obtained for LSZ (50% solvent) adsorbed onto silica in 10 mM phosphate buffer at pH 7.4.[36] Macakova et al. have previously shown that the amount of solvent sensed by QCM-D increases with the nanoscale roughness of the adsorbed layers.[23] In this study, it was also shown that the theoretically calculated solvent content expected for spherical micelles in a HCP arrangement is 39%, and for random sequential adsorption arrangements it is up to 63%. Hence, the predicted solvent content for adsorbed LSZ layers of this study (40−50%) is closer to a HCP layer than to a random layer, as discussed above.

3.3. Adsorption of Lysozyme Efficiently Hinders the Release of Silver at High Concentrations. From the QCM-D measurements it was evident that silver ions were released from the coated crystal directly upon exposure in pure $NaNO_3$ solution (Figure 4). The extent of released silver in $NaNO_3$ and the influence of the positively charged LSZ on the metal release process were hence investigated in 0.15 M $NaNO_3$ at pH 7 for massive silver surfaces. Silver is a relatively noble metal that, in contrast to most other metals, does not form any surface oxide at ambient conditions. A monolayer of atomic oxygen has rather been proposed to be reversibly adsorbed on the surface[46] whereas the silver oxide (Ag_2O) only is stable in a narrow region at highly alkaline (pH > 12) and oxidizing conditions.[47] The presence of physisorbed oxygen is supported by previous Raman measurements.[19] According to the Pourbaix digram is the silver metal generally stable in water but can dissolve to different extents (usually non-uniformly) at oxidizing conditions. The predominating corrosion products that form on silver in water of different pH and composition are Ag_2S and AgCl, which both possess large stability ranges in a wide pH interval. As sulfur-induced corrosion of silver in water and aqueous surface layers is believed to be the predominating process and partly proceed via the initial sorption of sulfur-containing functional groups, it is reasonable to assume that also the interaction between adsorbed LSZ (via disulfide bonds as previously discussed) and the silver surface will influence the corrosion and dissolution process.

The influence of LSZ on the released amount of silver in 0.15 M $NaNO_3$ (NA) is illustrated in Figure 7a. The surfaces were continuously exposed to pure $NaNO_3$ solutions in the absence and presence of 1 g/L LSZ during 2−24 h. Most silver is released during the first 2 h of exposure for both conditions. Even though the average value for $NaNO_3$ only implies an

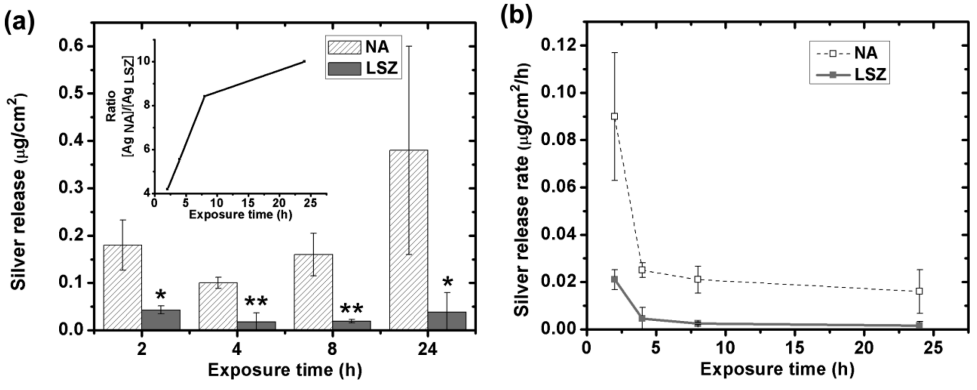

Figure 7. Cumulative released amounts (a) and average rates (based on the cumulative released amounts) (b) of silver versus time of exposure for massive silver in 0.15 M $NaNO_3$ (NA) and 0.15 M $NaNO_3$ containing 1 g/L LSZ. Asterisks indicate significant decrease of silver release in protein solution compared with pure $NaNO_3$, as calculated by Student's *t*-test, *p < 0.05, **p < 0.01. Inset: Ratio between released silver in the presence of LSZ and released silver in pure $NaNO_3$.

dx.doi.org/10.1021/la503170x | Langmuir 2014, 30, 13877−13889

increased released amount with time, this cannot be statistically proven. The large deviation between triplicate samples exposed for 24 h in $NaNO_3$ may imply non-uniform corrosion and dissolution as discussed above. However, as no surface analyses were made, this cannot be confirmed. Significantly lower released amounts of silver were though evident in the presence of LSZ for all time periods investigated. This suggests that the rapid adsorption process that firmly attaches LSZ to the silver surface (discussed in sections 3.1 and 3.2) results in a layer of efficient barrier properties that physically hinders the release of silver from the surface to solution, and/or that sulfur-containing corrosion products of poor solubility may form beneath the adsorbed LSZ bilayer. Improved barrier properties with time may be indicated by a 4-fold reduction in released amount of silver in the presence of LSZ compared with non-LSZ containing $NaNO_3$, after 2 h and a 10-fold reduction after 24 h. However, longer time periods need to be investigated to address this time effect, if any.

The average release rate of silver decreases strongly with time in both solutions with relatively steady-state rates of 0.016 $\mu g/cm^2/h$ in pure $NaNO_3$ and 0.0016 $\mu g/cm^2/h$ in $NaNO_3$ containing 1 g/L LSZ after 24 h (Figure 7b). A similar time-dependence has previously been observed for protein-induced metal release from stainless steel, an effect primarily attributed to improved barrier properties of the chromium-rich surface oxide with time.[8] This is not the case for silver, which does not form such a surface oxide. The initial higher release is rather related to the dissolution of reversibly adsorbed Ag−O.[8,48]

The protein concentration influences not only the adsorption process of LSZ onto the silver surface as previously discussed, but also the extent of released silver. Figure 8 displays the amount of released silver from massive silver after 2 and 24 h in pure $NaNO_3$ and $NaNO_3$ with different concentrations of LSZ (ranging from 0.01 to 1 g/L). Non-significant changes in the amount of released silver were observed compared with non-protein-containing $NaNO_3$ for LSZ concentrations less than 1 g/L. Increased released amounts of silver with time were shown to be statistically significant. Previous investigations suggest that the presence of protein in solution will contribute to the extent of metal release if the protein concentration in solution is high enough to enable the formation of a fully covered monolayer of adsorbed proteins.[8] Adsorption studies of this study reveal a non-fully covered surface of adsorbed LSZ at concentrations ≤0.1 g/L (Figure 5a). However, a bilayer with an inner firmly attached layer and a more loosely bound outer layer is proposed to form at the surface at the higher LSZ concentration (1 g/L) (Figure 6b). This proposed structure seems to effectively hinder the release of silver (Figure 8). This will be discussed in more detail in section 3.4.

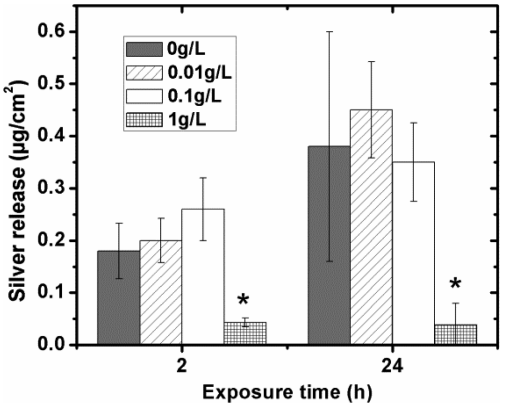

Figure 8. Released amount of silver from massive silver after 2 and 24 h exposure in solutions of increased LSZ concentration (0, 0.01, 0.1, and 1 g/L). Asterisks indicate significant decrease of silver release in protein solution compared with pure $NaNO_3$, as calculated by Student's *t*-test, $*p < 0.05$.

In order to elucidate the mechanism of silver release in more detail, silver surfaces were alternately exposed to LSZ (1 g/L) and/or LSZ-free $NaNO_3$ solutions measuring the amount of released silver in solution. The study focuses on the release of silver in different solutions during the first 3 h of exposure.

Total accumulated amounts of released silver after each step of the four solution sequences are displayed in Figure 9. The amount of released silver gradually increases with time upon exposure in the pure $NaNO_3$ sequence (Figure 9a). Released silver in the LSZ sequence reaches constant levels already after 1 h and, results in significantly lower released amounts of silver compared with the pure $NaNO_3$ sequence (Figure 9b). These findings are consistent with previous results (Figures 7a and 8). From the alternating exposures in LSZ and pure $NaNO_3$ solutions (Figure 9c,d), it is evident that the release of silver increases during steps with pure $NaNO_3$ solutions compared with LSZ steps. After 3 h the total amount of released silver is still lower for both alternating sequences compared with the pure $NaNO_3$ sequence but higher compared with the pure LSZ sequence. It should be emphasized that the amounts of silver released during these short exposure time periods (30 min) are relatively low and in many cases close to the LOQ, from which follows a variability of 5−10% between duplicate/triplicate samples (cf. Experimental Section). Above LOQ is the variability typically less than 2%. Measured concentrations close to LOQ hence mean that no absolute values can be determined, but that the given values have high enough accuracy to enable discrimination of trends. The absolute amount of released silver is therefore uncertain, but the trends of released silver in LSZ solutions and LSZ-free solutions are clearly shown.

3.4. Several Mechanisms Possible That Govern the Extent of Silver Release in the Presence of Lysozyme.

Several mechanisms have previously been proposed to explain protein induced metal release in the presence of proteins in solution.[8,11,49] The mechanisms include (i) surface complexation between proteins and metal ions and (ii) surface charge regulation resulting in the accumulation of counterions at the interface between the protein molecule and the metal surface. A possible mechanism for the release of silver in the presence of LSZ will be discussed in more detail below together in relation to the structure of the adsorbed protein layer and how that may influence the surface potential at the protein/solution interface and thereby have an effect on the release of metal ions into the surrounding solution.

3.4.1. Surface Complexation between LSZ and Silver Ions.

It is well known that proteins form complexes with metal ions and, soft metal ions rather than hard metal ions (according to the HSAB principle[50]) will selectively adsorb to proteins.[49] Silver ions are considered as soft and may coordinate with adsorbed LSZ molecules at the surface and with free protein molecules in the solution. Protein adsorption is a dynamic process, and proteins in the solution will exchange with proteins adsorbed at the surface.[7,35,51] During this exchange, detachment of silver−protein complexes may occur; however, this should result in an increased concentration of silver in the solution,

dx.doi.org/10.1021/la503170x | Langmuir 2014, 30, 13877−13889

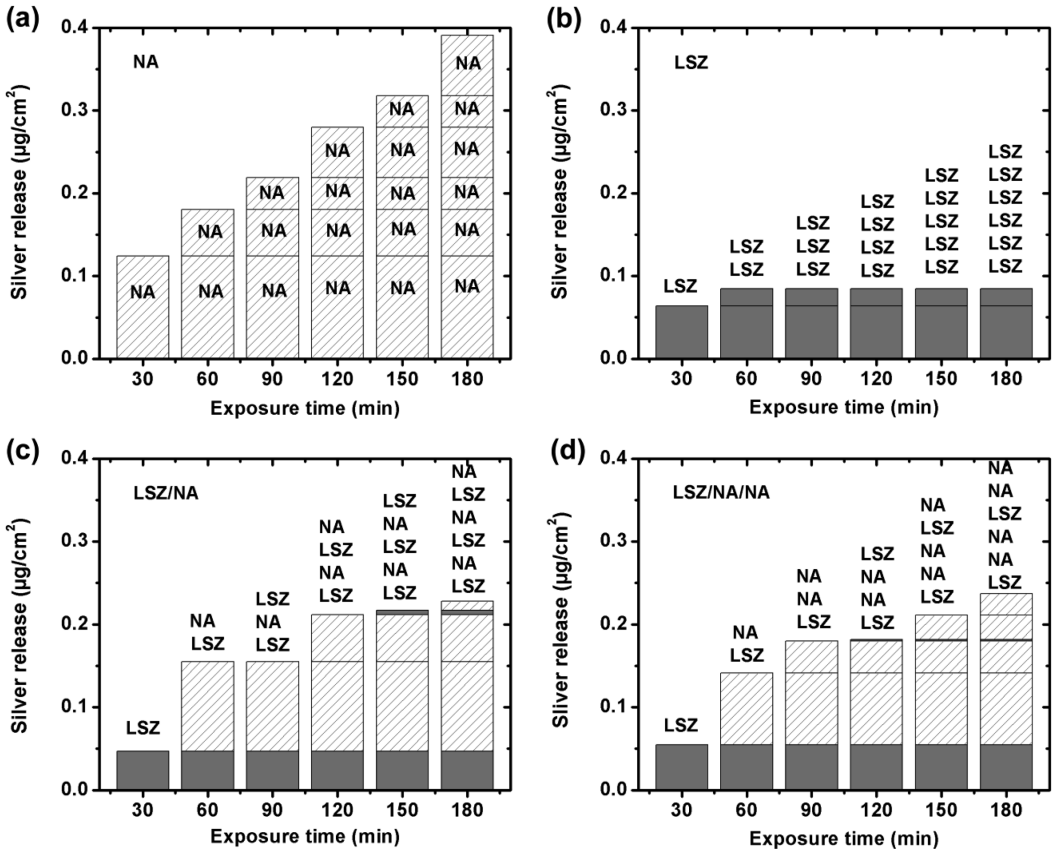

Figure 9. Total amounts of silver released from massive silver surfaces exposed to different $NaNO_3$ (NA) solution sequences, with and without LSZ (1 g/L) and for exposure periods ranging from 30 min to 3 h. The silver samples were kept in each solution for 30 min before transferred to the next solution. Samples were continuously exposed in "fresh" solution in 30 min cycles, following the sequences: (a) NA-NA-NA-NA-NA-NA, (b) LSZ-LSZ-LSZ-LSZ-LSZ-LSZ, (c) LSZ-NA-LSZ-NA-LSZ-NA, and (d) LSZ-NA-NA-LSZ-NA-NA. The procedure is schematically illustrated in section 2.6.2.

not observed in the present study. As discussed earlier, binding of LSZ to the silver surface is expected to be strong due to the interaction between disulfide bridges in the LSZ and the silver surface. This is expected to reduce the exchange rate between adsorbed proteins at the surface and in the solution.[51] Proteins are generally regarded as irreversibly adsorbed with respect to dilution with a protein-free electrolyte, and the exchange with proteins in solution will be terminated, along with any possible detachment of silver−LSZ complexes.

3.4.2. Surface Charge Regulation and Apparent Surface Potential at the Protein/Solution Interface. Zeta potential measurements revealed that the silver surface is negatively charged at pH 7 in 1 mM $NaNO_3$ (Figure 1). Electroneutrality requires that the net surface charge (surface potential) outside a charged surface is balanced by ions in the Stern layer (counterions) and the electrical double-layer made up from both counterions and co-ions in rapid thermal motion.[6] The distribution of the ions at the surface can be calculated using the Boltzmann distribution for the different ions. When considering the proton concentration outside a charged surface, it is evident from the Boltzmann distribution that the surface pH (as well as the protein surface pH) differs from the bulk pH (unless the surface potential is zero).[52,53] Proton concentration at a negatively charged surface will be higher compared to in bulk giving a local lower pH close to the surface. However, for a zeta potential of −30 mV at pH 7, only a slight reduction to pH 6.5 will be obtained without taking into account any adsorption of counterions from 0.15 M $NaNO_3$, which will probably have a significant effect of the lowering of the surface pH. This indicates that a local decrease in pH at the surface will not contribute to a large extent to the release of silver from the surface in pure electrolyte solution at pH 7.

When two charged objects (e.g., the charged silver surface and the charged LSZ) come in close proximity of each other and the charges do not match, adsorption would result in an accumulation of the net charge in the interfacial region between the surface and the protein. Since the dielectric permittivity (ε) is lower in the adsorbed protein layer compared to the bulk electrolyte solution, accumulation of charges is unfavorable. However, electroneutrality implies that ions from the solution will be transported from solution to compensate the accumulation of net charge,[54,55] and at smaller separations, this charge regulation effect will be more significant.[56] In the present study, Na^+ and NO_3^- will be incorporated in the interfacial region, and the amount will depend on the charge of the surface and the protein, respectively. Released Ag^+ from the silver surface can contribute to the charge regulation in the interfacial layer. It may also form a complex with NO_3^-; however, these complexes are highly soluble and will not contribute to the reduction of silver ions in the solution via precipitation of insoluble silver complexes.

If the structure of the adsorbed layer is considered, it was discussed earlier that the protein concentration in solution influences the adsorbed mass of adsorbed LSZ layer on the silver surface. At a LSZ concentration of 1 g/L, a bilayer structure was obtained, i.e., a denser inner layer and an outer less dense layer.

dx.doi.org/10.1021/la503170x | *Langmuir* 2014, 30, 13877−13889

When considering the charge distribution within the LSZ layer, it can be viewed as a three-layer model proposed by Norde et al.[7,57] In the inner region (1), with a thickness in the order of the diameter of a hydrated ion (a few tenths of a nanometer), any mismatch of LSZ and silver charge in this region between the silver surface and the inner LSZ layer is compensated by electrolyte ions to make this region nearly electrically neutral. The central region (2) is analogous to the interior of the native state of LSZ (with low dielectric permittivity) and is considered to be voids of isolated charged groups and oppositely charged groups may occur in ion pairs. Thus, the volume charge density in this region is zero. In region (3), the protein/solution interface, the charged groups on the LSZ are exposed toward the electrolyte solution (0.15 m $NaNO_3$) giving rise to a charged surface. Since this region extends to the shear plane, it will also accommodate ions bound in the Stern layer of adsorbed LSZ molecules. The thickness equals to the sum of hydration layer thickness and an outer shell, accommodating free charges, of the LSZ layer.

When considering the structure of the adsorbed LSZ layer on the silver surface, i.e., a bilayer structure in the case of 1 g/L LSZ in solution, a net interfacial charge reversal is expected due to the presence of positively charged LSZ molecules in the loosely bound outer layer. Hence, a net positive surface potential would be obtained at the LSZ/solution interface. This has previously been found experimentally for LSZ adsorption on negatively charged silica and mica.[44,58] For LSZ adsorption on silica, a net interfacial charge reversal was found for all examined ionic strengths. The same was found for LSZ adsorption on a negatively modified alumina surface, where an alteration of the measured zeta potential from negative to weak positive was obtained.[59] A charge reversal was also proposed based on mathematical arguments caused by a second protein layer adsorbed on the first layer onto metal surfaces.[51] In the present study, it might be argued that the presence of an outer layer of LSZ at the highest protein concentration (1 g/L) could induce a charge reversal resulting in a positive interfacial potential at the protein solution interface. Any released silver ions from the surface would then exhibit an electrostatic repulsion during transport through the protein layer and, hence, a reduced amount of ions in the surrounding solution will be obtained. This also in accordance with the fact that an increased release is obtained after rinsing in pure 0.15 M $NaNO_3$ (see Figure 9c,d), where the outer protein layer is removed and a decrease of the net interfacial potential can be anticipated which will decrease the electrostatic repulsion for the silver ions during the transport through the protein layer. Hence, an increased release of Ag^+ can be expected in pure electrolyte solution even though a layer of LSZ remains on the silver surface. It should be kept in mind that the adsorbed LSZ layer does not fully cover the silver surface, as discussed earlier and, therefore voids between the protein molecules are present that allow ions to diffuse through the layer.[44] When the samples are repeatedly immersed in 1 g/L LSZ, re-adsorption of the outermost layer will occur and, hence, the silver release will decrease again. The above discussion can also explain the absence of reduced silver release at lower protein concentrations, where adsorption of a second layer of LSZ is not observed.

4. CONCLUSION

A comprehensive investigation of LSZ adsorption was performed on silver surfaces using a combined ellipsometry and QCM-D module allowing in real-time and simultaneous measurements of the adsorbed amount ("dry mass") and the sensed mass ("wet mass") on the very same surface, to obtain a detailed interpretation of the layer structure, rigidity, and its solvent content. As expected, the protein concentration significantly influences the structure of the adsorbed layer. A non-fully surface-covered rigid layer forms at concentrations, ≤0.1 g/L, with most molecules packed side-on in a monolayer arrangement, whereas a bilayer conformation is obtained at high concentrations (1 g/L). The inner layer is assumed to be firmly bound to the silver surface via disulfide bridges, whereas the outer layer forms loosely and is easily desorbed by dilution with a protein-free solution. The layer viscosity and layer shear elastic modulus, calculated by Voigt, are increased after rinsing, which implies increasingly more rigid layers during rinsing due to partial desorption of the outer loosely bound layer. The fact that the layer viscosity and the layer shear modulus increase with increased LSZ concentration indicates a tighter packed layer at higher concentration. This may be related to a more extensive adsorption of LSZ onto the silver-coated surface.

The extent of released silver in $NaNO_3$ and the influence of the positively charged LSZ on the metal release process were investigated for massive silver surfaces using GF-AAS. Adsorption of LSZ efficiently hinders the release of silver at high concentration. Improved barrier properties with time may be indicated by a 4-fold reduction in released amount of silver in the presence of LSZ after 2 h compared with non-LSZ containing $NaNO_3$, and a 10-fold reduction after 24 h. The protein concentration influences the extent of released silver. Non-significant changes in the amount of released silver were observed compared with non-protein-containing $NaNO_3$ for LSZ concentrations less than 1 g/L. Further, it is evident that the reduction of silver release only took place at higher LSZ concentrations, which may be an indication of the necessity of a bilayer configuration.

Several mechanisms to explain the extent of silver release in the presence of LSZ are possible. In this study the results points to that the most plausible mechanism to explain reduced amounts of released silver in the presence of bilayer structure of adsorbed LSZ is the existence of a repulsive electrostatic barrier at the protein/solution interface (positive interfacial potential) for released silver ions. This would reduce the transport of the silver ions through the protein layer and, hence, a reduced amount of ions released into the surrounding solution. This also in accordance with increased released amounts of silver observed after rinsing (in pure 0.15 M $NaNO_3$), which results in the removal of the outer protein layer and an anticipated reduction in net interfacial potential that will decrease the electrostatic repulsion for the silver ions.

AUTHOR INFORMATION

Corresponding Author

*Eva Blomberg, e-mail: blev@kth.se. Xin Wang, e-mail: xiwa@kth.se.

Notes

The authors declare no competing financial interest.

ACKNOWLEDGMENTS

The Chinese Scholarship Council (CSC) is gratefully acknowledged for the financial support of X.W. Financial support from the Swedish National Research Councils (VR) is highly acknowledged. The authors thank Dr. Maria Lundin Johnson and Sara Skoglund for kindly providing zeta potential and contact angle data for the silver-coated QCM-D crystal and the

massive silver surfaces. Dr. Yolanda Hedberg and Dr. Jonas Hedberg are acknowledged for valuable help with evaluating the amount of silver released using GF-AAS. Dr. Lubica Macakova is acknowledged for valuable discussions and help with ellipsometry measurements and data analysis.

REFERENCES

(1) Silver, S.; Phung, L.; Silver, G. Silver as biocides in burn and wound dressings and bacterial resistance to silver compounds. *J. Ind. Microbiol. Biotechnol.* **2006**, *33*, 627−634.
(2) Marambio-Jones, C.; Hoek, E. V. A review of the antibacterial effects of silver nanomaterials and potential implications for human health and the environment. *J. Nanopart. Res.* **2010**, *12*, 1531−1551.
(3) Poulter, N.; Vasilev, K.; Griesser, S.; Griesser, H., Silver Containing Biomaterials. In *Biomaterials Associated Infection*; Moriarty, T. F., Zaat, S. A. J., Busscher, H. J., Eds.; Springer: New York, 2013; pp 355−378.
(4) Agnihotri, S.; Mukherji, S.; Mukherji, S. Immobilized silver nanoparticles enhance contact killing and show highest efficacy: elucidation of the mechanism of bactericidal action of silver. *Nanoscale* **2013**, *5*, 7328−7340.
(5) Claesson, P. M.; Blomberg, E.; Fröberg, J. C.; Nylander, T.; Arnebrant, T. Protein interactions at solid surfaces. *Adv. Colloid Interface Sci.* **1995**, *57*, 161−227.
(6) Haynes, C. A.; Norde, W. Globular proteins at solid/liquid interfaces. *Colloids Surf., B* **1994**, *2*, 517−566.
(7) Norde, W. My voyage of discovery to proteins in flatland... and beyond. *Colloids Surf., B* **2008**, *61*, 1−9.
(8) Hedberg, Y.; Wang, X.; Hedberg, J.; Lundin, M.; Blomberg, E.; Wallinder, I. O. Surface-protein interactions on different stainless steel grades: effects of protein adsorption, surface changes and metal release. *J. Mater. Sci.: Mater. Med.* **2013**, *24*, 1015−1033.
(9) Sugiyama, H.; Hagiwara, T.; Watanabe, H.; Sakiyama, T. Effects of ionic substances on the adsorption of egg white proteins to a stainless steel surface. *Biosci., Biotechnol., Biochem.* **2010**, *76*, 467−472.
(10) Gispert, M. P.; Serro, A. P.; Colaco, R.; Saramago, B. Bovine serum albumin adsorption onto 316L stainless steel and alumina: a comparative study using depletion, protein radiolabeling, quartz crystalmicrobalance and atomic force microscopy. *Surf. Interface Anal.* **2008**, *40*, 1529−1537.
(11) Lundin, M.; Hedberg, Y.; Jiang, T.; Herting, G.; Wang, X.; Thormann, E.; Blomberg, E.; Wallinder, I. O. Adsorption and protein-induced metal release from chromium metal and stainless steel. *J. Colloid Interface Sci.* **2012**, *366*, 155−164.
(12) Hansen, D. C.; Luther Iii, G. W.; Waite, J. H. The Adsorption of the Adhesive Protein of the Blue Mussel Mytilus edulis L onto Type 304L Stainless Steel. *J. Colloid Interface Sci.* **1994**, *168*, 206−216.
(13) Imoto, T.; Johnson, I. N.; North, A. C. T.; Phillips, D. C.; Rupley, J. A., Vertevrate lysozymes. In *The Enzymes*, 3rd ed.; Boyer, P., Ed.; Academic Press: New York, 1972; Vol. 7.
(14) Hankiewicz, J.; Swierczek, E. Lysozyme in human body fluids. *Clin. Chim. Acta* **1974**, *57*, 205−209.
(15) Luxbacher, T. Electrokinetic characterization of flat sheet membranes by streaming current measurement. *Desalination* **2006**, *199*, 376−377.
(16) Xie, H.; Saito, T.; Hickner, M. A. Zeta Potential of Ion-Conductive Membranes by Streaming Current Measurements. *Langmuir* **2011**, *27*, 4721−4727.
(17) Sotiriou, G. A.; Meyer, A.; Knijnenburg, J. T. N.; Panke, S.; Pratsinis, S. E. Quantifying the Origin of Released Ag+ Ions from Nanosilver. *Langmuir* **2012**, *28*, 15929−15936.
(18) Han, Y.; Lupitskyy, R.; Chou, T.-M.; Stafford, C. M.; Du, H.; Sukhishvili, S. Effect of Oxidation on Surface-Enhanced Raman Scattering Activity of Silver Nanoparticles: A Quantitative Correlation. *Anal. Chem.* **2011**, *83*, 5873−5880.
(19) Hedberg, J.; Lundin, M.; Lowe, T.; Blomberg, E.; Wold, S.; Wallinder, I. O. Interactions between surfactants and silver nanoparticles of varying charge. *J. Colloid Interface Sci.* **2012**, *369*, 193−201.
(20) Rodahl, M.; Höök, F.; Krozer, A.; Brzezinski, P.; Kasemo, B. Quartz crystal microbalance setup for frequency and Q-factor measurements in gaseous and liquid environments. *Rev. Sci. Instrum.* **1995**, *66*, 3924−3930.
(21) Sauerbrey, G. Verwendung von Schwingquarzen zur Wägung dünner Schichten und zur Mikrowägung. *Z. Phys.* **1959**, *155*, 206−222.
(22) Voinova, M. V.; Rodahl, M.; Jonson, M.; Kasemo, B. Viscoelastic acoustic response of layered polymer films at fluid-solid interfaces: continuum mechanics approach. *Phys. Scr.* **1999**, *59*, 391−396.
(23) Macakova, L.; Blomberg, E.; Claesson, P. M. Effect of Adsorbed Layer Surface Roughness on the QCM-D Response: Focus on Trapped Water. *Langmuir* **2007**, *23*, 12436−12444.
(24) De Feijter, J. A.; Benjamins, J.; Veer, F. A. Ellipsometry as a tool to study the adsorption behavior of synthetic and biopolymers at the air−water interface. *Biopolymer* **1978**, *17*, 1759−1772.
(25) Vörös, J. The density and refractive index of adsorbing protein layers. *Biophys. J.* **2004**, *87*, 553−561.
(26) Mertens, F. P.; Theroux, P.; Plumb, R. C. Some Observations on the Use of Elliptically Polarized Light to Study Metal Surfaces. *J. Opt. Soc. Am.* **1963**, *53*, 788−793.
(27) Halthur, T. J.; Elofsson, U. M. Multilayers of Charged Polypeptides As Studied by in Situ Ellipsometry and Quartz Crystal Microbalance with Dissipation. *Langmuir* **2004**, *20*, 1739−1745.
(28) Vogelsang, J.; Hädrich, J. Limits of detection, identification and determination: a statistical approach for practitioners. *Accredit. Qual. Assur.* **1998**, *3*, 242−255.
(29) Chandrasekaran, N.; Dimartino, S.; Fee, C. J. Study of the adsorption of proteins on stainless steel surfaces using QCM-D. *Chem. Eng. Res. Des.* **2013**, *91*, 1674−1683.
(30) Ramsden, J. J. Puzzles and paradoxes in protein adsorption. *Chem. Soc. Rev.* **1995**, *24*, 73−78.
(31) Imamura, K.; Mimura, T.; Okamoto, M.; Sakiyama, T.; Nakanishi, K. Adsorption Behavior of Amino Acids on a Stainless Steel Surface. *J. Colloid Interface Sci.* **2000**, *229*, 237−246.
(32) Evans, D. F.; Wennerström, H. *The Colloidal Domain: Where Physics, Chemistry, Biology, and Technology Meet*, 2nd ed.; Wiley-VCH: New York, 1999.
(33) Henzler, K.; Haupt, B.; Lauterbach, K.; Wittemann, A.; Borisov, O.; Ballauff, M. Adsorption of *β*-Lactoglobulin on Spherical Polyelectrolyte Brushes: Direct Proof of Counterion Release by Isothermal Titration Calorimetry. *J. Am. Chem. Soc.* **2010**, *132*, 3159−3163.
(34) Podstawka, E.; Ozaki, Y.; Proniewicz, L. M. Adsorption of S-S Containing Proteins on a Colloidal Silver Surface Studied by Surface-Enhanced Raman Spectroscopy. *Appl. Spectrosc.* **2004**, *58*, 1147−1156.
(35) Brash, J. L.; Samak, Q. M. Dynamics of interactions between human albumin and polyethylene surface. *J. Colloid Interface Sci.* **1978**, *65*, 495−504.
(36) Xu, K. R.; Ouberai, M. M.; Welland, M. E. A comprehensive study of lysozyme adsorption using dual polarization interferometry and quartz crystal microbalance with dissipation. *Biomaterials* **2013**, *34*, 1461−1470.
(37) Su, T. J.; Lu, J. R.; Thomas, R. K.; Cui, Z. F.; Penfold, J. The Effect of Solution pH on the Structure of Lysozyme Layers Adsorbed at the Silica-Water Interface Studied by Neutron Reflection. *Langmuir* **1998**, *14*, 438−445.
(38) Tilton, R. D.; Blomberg, E.; Claesson, P. M. Effect of anionic surfactant on interactions between lysozyme layers adsorbed on mica. *Langmuir* **1993**, *9*, 2102−2108.
(39) Höök, F.; Rodahl, M.; Kasemo, B.; Brzezinski, P. Structural changes in hemoglobin during adsorption to solid surfaces: Effects of pH, ionic strength, and ligand binding. *Proc. Natl. Acad. Sci. U.S.A.* **1998**, *95*, 12271−12276.
(40) Shen, D.; Huang, M.; Chow, L.-M.; Yang, M. Kinetic profile of the adsorption and conformational change of lysozyme on self-assembled monolayers as revealed by quartz crystal resonator. *Sens. Actuators, B* **2001**, *77*, 664−670.

(41) Lu, J. R.; Swann, M. J.; Peel, L. L.; Freeman, N. J. Lysozyme Adsorption Studies at the Silica/Water Interface Using Dual Polarization Interferometry. *Langmuir* **2004**, *20*, 1827−1832.
(42) Plunkett, M. A.; Claesson, P. M.; Ernstsson, M.; Rutland, M. W. Comparison of the Adsorption of Different Charge Density Polyelectrolytes: A Quartz Crystal Microbalance and X-ray Photoelectron Spectroscopy Study. *Langmuir* **2003**, *19*, 4673−4681.
(43) Dolatshahi-Pirouz, A.; Rechendorff, K.; Hovgaard, M. B.; Foss, M.; Chevallier, J.; Besenbacher, F. Bovine serum albumin adsorption on nano-rough platinum surfaces studied by QCM-D. *Colloids Surf., B* **2008**, *66*, 53−59.
(44) Blomberg, E.; Claesson, P. M.; Froberg, J. C.; Tilton, R. D. Interaction between adsorbed layers of lysozyme studied with the surface force technique. *Langmuir* **1994**, *10*, 2325−2334.
(45) Xie, Y.; Zhou, J.; Jiang, S. Parallel tempering Monte Carlo simulations of lysozyme orientation on charged surfaces. *J. Chem. Phys.* **2010**, *132*, 065101-1−065101-8.
(46) Czanderna, A. W. The Adsorption of Oxygen on Silver. *J. Phys. Chem.* **1964**, *68*, 2765−2771.
(47) Graedel, T. E. Corrosion Mechanisms for Silver Exposed to the Atmosphere. *J. Electrochem. Soc.* **1992**, *139*, 1963−1970.
(48) Hiemstra, T.; van Riemsdijk, W. H. Multiple activated complex dissolution of metal (hydr) oxides: A thermodynamic approach applied to quartz. *J. Colloid Interface Sci.* **1990**, *136*, 132−150.
(49) Saha, B.; Chakraborty, S.; Das, G. A Rational Approach for Controlled Adsorption of Metal Ions on Bovine Serum Albumin−Malachite Bionanocomposite. *J. Phys. Chem. C* **2010**, *114*, 9817−9825.
(50) Pearson, R. G. Hard and Soft Acids and Bases. *J. Am. Chem. Soc.* **1963**, *85*, 3533−3539.
(51) Lundström, I. Models of protein adsorption on solid surfaces. *Prog. Colloid Polym. Sci.* **1985**, *70*, 76−82.
(52) Boström, M.; Deniz, V.; Franks, G. V.; Ninham, B. W. Extended DLVO theory: Electrostatic and non-electrostatic forces in oxide suspensions. *Adv. Colloid Interface Sci.* **2006**, *123*−*126*, 5−15.
(53) Boström, M.; Tavares, F. W.; Finet, S.; Skouri-Panet, F.; Tardieu, A.; Ninham, B. W. Why forces between proteins follow different Hofmeister series for pH above and below pI. *Biophys. Chem.* **2005**, *117*, 217−224.
(54) Fraaije, J. G. E. M.; Murris, R. M.; Norde, W.; Lyklema, J. Interfacial thermodynamics of protein adsorption, ion co-adsorption and ion binding in solution: I. Phenomenological linkage relations for ion exchange in lysozyme chromatography and titration in solution. *Biophys. Chem.* **1991**, *40*, 303−315.
(55) Fraaije, J. G. E. M.; Norde, W.; Lyklema, J. Interfacial thermodynamics of protein adsorption and ion co-adsorption. III. Electrochemistry of bovine serum albumin adsorption on silver iodide. *Biophys. Chem.* **1991**, *41*, 263−276.
(56) Grant, M. L. Nonuniform Charge Effects in Protein−Protein Interactions. *J. Phys. Chem. B* **2001**, *105*, 2858−2863.
(57) Norde, W.; Lyklema, J. The adsorption of human plasma albumin and bovine pancreas ribonuclease at negatively charged polystyrene surfaces: IV. The charge distribution in the adsorbed state. *J. Colloid Interface Sci.* **1978**, *66*, 285−294.
(58) Daly, S. M.; Przybycien, T. M.; Tilton, R. D. Coverage-dependent orientation of lysozyme adsorbed on silica. *Langmuir* **2003**, *19*, 3848−3857.
(59) Saha, B.; Saikiab, J.; Das, G. Tuning the selective interaction of lysozyme and serum albumin on a carboxylate modified surface. *RSC Adv.* **2013**, *3*, 7867−7879.